Karttunen, Anssi T.; Von Hertzen, Raimo

On the foundations of anisotropic interior beam theories

Published in:
Composites Part B: Engineering

DOI:
10.1016/j.compositesb.2015.10.026

Published: 15/02/2016

Document Version
Peer reviewed version

On the foundations of anisotropic interior beam theories

Anssi T. Karttunen[a,*], Raimo von Hertzen[a]

[a]*Department of Applied Mechanics, Aalto University, Finland*

Abstract

This study has two main objectives. First, we use the Airy stress function to derive an exact general interior solution for an anisotropic two-dimensional (2D) plane beam. Second, we cast the solution into the conventional form of 1D beam theories to clarify some basic concepts related to anisotropic interior beams. The derived general solution provides the exact third-order interior kinematic description for the plane beam and includes the Levinson/Reddy–kinematics as a special case. By applying the Clapeyron's theorem, we show that the stresses acting as surface tractions on the lateral end surfaces of the interior beam need to be taken into account in all energy-based considerations related to the interior beam in order to avoid artificial end effects. Exact 1D interior beam equations are formed from the general 2D solution. Finally, we develop an exact interior beam finite element based on the general solution. With full anisotropic coupling, the stiffness matrix of the element becomes initially asymmetric due to the interior nature of the plane beam. By redefining the generalized nodal axial forces of the element, the stiffness matrix takes a symmetric form.

Keywords: B. Anisotropy, B. Elasticity, C. Analytical Modelling, C. Finite element analysis (FEA)

1. Introduction

Efficient use of anisotropic composite materials in mechanical design requires thorough understanding of anisotropic elasticity and accurate tools of analysis. Motivated by this, we study here a two-dimensional (2D) plane beam with anisotropic coupling effects within the framework of 2D linear elasticity.

There are two well-known complex variable formulations for 2D linearly elastic anisotropic plane problems, the Lekhnitskii and Stroh formalisms [1–3]. When it comes to 2D interior plane beam problems, where the end effects are neglected by virtue of the Saint Venant's principle, a number of more straightforward polynomial-based stress function approaches can be found in the literature, e.g. [4–6]. It is common for these classical polynomial approaches that a solution is generated only for one problem at a time. In this study, we first provide a more versatile method for 2D beams which is based on a general interior solution derived using the Airy stress function. Our approach is different from the generalization of Silverman's method [4] by Ding et al. [7] in the way that, rather than constructing stress functions for each problem separately, the focus is on solving the cross-sectional force and moment resultants along a beam for each case in the same way as in conventional beam theories, while the core of the used stress function is always the same.

There is a number of ingenious theories meant specifically for anisotropic beams, e.g. [8–13]. For a historical survey on the topic, see the book by Hodges [14]. The mentioned anisotropic beam theories are typically applicable to a wider variety of practical problems than the linearly elastic beam with a rectangular cross-section studied in this paper. However, it is commonplace in the referenced treatments to employ engineering assumptions and/or to rely on a quite heavy theoretical machinery. Therefore, it is often difficult to see the underlying structure of the developments in a fully explicit (and assumption-free) form in order to state something fundamental on anisotropic beams in general. Thus, for the remainder of this

Recompiled, unedited accepted manuscript. **Cite as**: *Compos. Part B-Eng.* 2016;87:299–310. doi link
*Corresponding author. *anssi.karttunen@iki.fi*

study, we view the derived 2D solution for the anisotropic plane beam as a conventional one-dimensional (1D) beam theory in order to clarify certain concepts related to anisotropic interior beams.

As the starting point for the 1D considerations, the general solution provides the exact third-order interior kinematic description for the plane beam. By "third-order kinematics" we mean that the displacement components defined at the central axis of the beam are expanded by third-order polynomials throughout the height of the beam. Many approximate beam and plate theories, which are used also in association with anisotropic composite materials, are based on similar, but assumed, displacement fields. For reviews on assumed third-order kinematics, see the works by Jemielita [15] and Reddy [16, 17]. The exact interior kinematic description derived from the general solution in this paper includes, as a special case, the displacement field which is used to derive the widely known Levinson and Reddy–Bickford beam theories [18–20].

The long-standing belief in the literature is that the Levinson beam theory is "variationally inconsistent", that is to say, it cannot be derived using the principle of virtual displacements. In contrast to this, we showed in a very recent study that the Levinson theory is actually variationally consistent [21]. The variational formulation was carried out by taking into account the fact that the stresses of the beam act as surface tractions on the lateral end surfaces of the Levinson beam. On the other hand, it was shown that the boundary layer behavior of the Reddy–Bickford beam is artificial. In the present study, the methodology utilized for the isotropic Levinson theory in [21] is further elucidated within the 2D interior framework of anisotropic elasticity.

The rest of the paper is organized in the following way. In Section 2, we formulate the anisotropic plane beam problem to which the solution is then given in terms of a stress function. The strains are calculated from the stresses under plane stress conditions and the exact 2D interior displacement field is obtained by integrating the strains. Calculation examples are presented. In Section 3, three kinematic variables defined at the central axis of the plane beam are formed from the 2D interior displacement field. Using these variables, the third-order kinematic description for the beam is given. Clapeyron's theorem is employed to facilitate energy-based considerations. Variational and vectorial approaches for interior theories are discussed and finally 1D beam equations for the 2D plane beam are obtained by a direct method. In Section 4, an exact interior beam finite element is developed both by a force-based method and from the total potential energy of the anisotropic plane beam. Conclusions are presented in Section 5.

2. General interior approach for a plane beam

2.1. Problem formulation

A 2D linearly elastic homogeneous anisotropic plane beam under a uniform pressure p is shown in Fig. 1. We have chosen the uniform load as a representative load for our developments. The beam has a rectangular cross-section of constant thickness t and the length and height of the beam are L and h, respectively. The load resultants N, M and Q stand for the axial force, bending moment and shear force, respectively, and act at an arbitrary cross-section of the beam. These cross-sectional load resultants are calculated from

$$N(x) = t\int_{-h/2}^{h/2} \sigma_x dy \ , \quad M(x) = t\int_{-h/2}^{h/2} \sigma_x y dy \ , \quad Q(x) = t\int_{-h/2}^{h/2} \tau_{xy} dy \ , \tag{1}$$

which can be used to impose force and moment boundary conditions at $x = \pm L/2$. The boundary conditions on the upper and lower surfaces of the plane beam are

$$\sigma_y(x, h/2) = -p \ , \qquad \sigma_y(x, -h/2) = 0 \ , \qquad \tau_{xy}(x, \pm h/2) = 0 \ . \tag{2}$$

The boundary conditions are satisfied in a *strong* (pointwise) sense on the upper and lower surfaces, but at the beam ends the tractions are specified only through the load resultants and, thus, the boundary conditions are imposed only in a *weak* sense [22]. The replacement of the true boundary conditions at the beam ends by the statically equivalent weak boundary conditions (load resultants) means that the exponentially decaying end effects of the anisotropic plane beam are neglected by virtue of the Saint Venant's principle and only

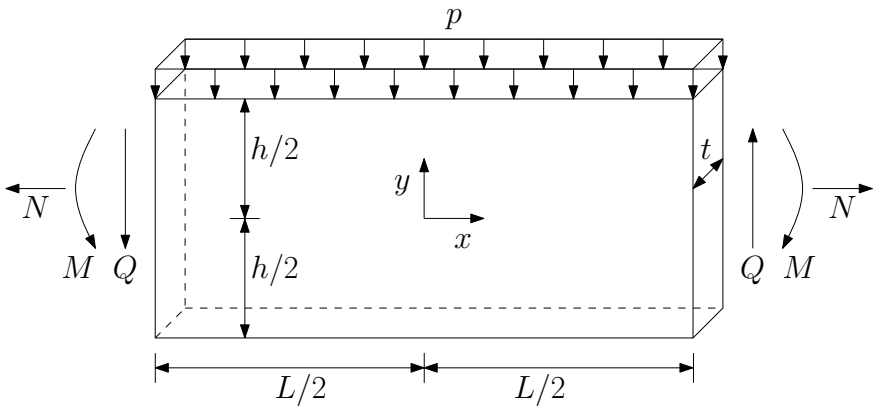

Figure 1: 2D anisotropic plane beam under a constant uniform pressure. The load resultants act at an arbitrary cross-section of the beam. The positive directions of the load resultants are defined for later use in calculation examples and finite element developments.

the interior solution of the beam is under consideration. The interior solution represents actually a beam section with fully-developed interior stresses which has been cut off from a complete beam far enough from the real lateral boundaries at which the true boundary conditions could be set. Using the Airy stress function $\Psi(x, y)$, the stresses of the plane beam are obtained from the equations

$$\sigma_x = \frac{\partial^2 \Psi}{\partial y^2}, \qquad \sigma_y = \frac{\partial^2 \Psi}{\partial x^2}, \qquad \tau_{xy} = -\frac{\partial^2 \Psi}{\partial x \partial y} \,, \tag{3}$$

which satisfy the two-dimensional equilibrium equations. To ensure compatibility, it is required that the stress function satisfies the governing equation [23]

$$s_{22}\frac{\partial^4 \Psi}{\partial x^4} - 2s_{26}\frac{\partial^4 \Psi}{\partial x^3 \partial y} + 2(s_{12} + s_{66})\frac{\partial^4 \Psi}{\partial x^2 \partial y^2} - 2s_{16}\frac{\partial^4 \Psi}{\partial x \partial y^3} + s_{11}\frac{\partial^4 \Psi}{\partial y^4} = 0 \,, \tag{4}$$

where s_{ij} are the elastic compliances, see Eqs. (15)–(17). The solution to the interior plane beam problem is obtained by finding a solution of Eq. (4) that satisfies the stress boundary conditions (2) of the beam.

2.2. Interior stresses

By starting from the general polynomial of the fifth degree and adapting a solution procedure outlined by Barber [22, Chap. 5] to solve the polynomial coefficients, the stress function satisfying the stress boundary conditions (2) can be found as

$$\Psi(x, y) = \; c_1 y^2 + c_2 y^3 - c_3 \left(\frac{3}{4} h^2 xy - xy^3 - \frac{1}{2} \frac{s_{16}}{s_{11}} y^4 \right) + \Psi_q \,, \tag{5}$$

where c_1, c_2 and c_3 are constant coefficients and the part that depends on the nature of the applied load is

$$\begin{aligned} \Psi_q = {} & \frac{q}{240I} \left[8\frac{s_{16}^2}{s_{11}^2} y^5 - 5x^2(h - y)(h + 2y)^2 \right] \\ & - \frac{q}{120 I s_{11}} \left[2s_{12} y^5 + 5s_{16}(h^2 - 2y^2)xy^2 + s_{66} y^5 \right] , \end{aligned} \tag{6}$$

where $q = pt$ is the uniform line load and $I = th^3/12$ is the second moment of the cross-sectional area. The stresses are calculated from Eqs. (3), after which the load resultants are obtained from Eqs. (1) and can be

written as

$$N(x) = 2Ac_1 + 6Ic_3\frac{s_{16}}{s_{11}} \ , \tag{7}$$

$$M(x) = 6I(c_2 + c_3x) + \frac{q}{40s_{11}^2}\left[20s_{11}^2x^2 + h^2(4s_{16}^2 - 2s_{11}s_{12} + s_{11}s_{66})\right] \ , \tag{8}$$

$$Q(x) = 6Ic_3 + qx \ , \tag{9}$$

where $A = ht$ is the area of the cross-section. The load resultants satisfy the global equilibrium equations

$$\frac{\partial N(x)}{\partial x} = 0 \ , \qquad \frac{\partial M(x)}{\partial x} = Q(x) \ , \qquad \frac{\partial Q(x)}{\partial x} = q \ . \tag{10}$$

Note that due to the anisotropic coupling term s_{16} in Eq. (7), the stretching of the beam is not uncoupled from the shearing. Furthermore, using Eqs. (7) and (9), we can write

$$N(x) = 2Ac_1 + \frac{s_{16}}{s_{11}}\left[Q(x) - qx\right] \ . \tag{11}$$

By solving Eqs. (7)–(9) for c_1, c_2 and c_3, the stresses (3) calculated using the stress function (5) are obtained in the form

$$\begin{aligned}\sigma_x = \ & \frac{N(x)}{A} + \frac{M(x)y}{I} - \frac{Q(x)}{A}\frac{s_{16}}{s_{11}}\left(1 - 12\frac{y^2}{h^2}\right) \\ & + \left(\frac{2s_{12} + s_{66}}{s_{11}} - 4\frac{s_{16}^2}{s_{11}^2}\right)\left(\frac{3qy}{10A} - \frac{qy^3}{6I}\right) \ ,\end{aligned} \tag{12}$$

$$\sigma_y = \ -\frac{q}{24I}\left(h^3 + 3h^2y - 4y^3\right) \ , \tag{13}$$

$$\tau_{xy} = \ \left[Q(x) + \frac{2}{3}\frac{s_{16}}{s_{11}}qy\right]\frac{h^2 - 4y^2}{8I} \ . \tag{14}$$

Indeed, when compared to an isotropic case, a marked effect due to the anisotropy is that the shear force $Q(x)$ appears in the axial stress (12). The above interior stress distributions are valid for any plane beam with a rectangular cross-section. To obtain stress distributions for other loads, one needs to update only the load-dependent part (6) of the stress function (5).

2.3. Interior strains and displacements

Under plane stress, that is, for a beam with a narrow rectangular cross-section, the stress-strain relations read

$$\epsilon_x = s_{11}\sigma_x + s_{12}\sigma_y + s_{16}\tau_{xy} \ , \tag{15}$$

$$\epsilon_y = s_{12}\sigma_x + s_{22}\sigma_y + s_{26}\tau_{xy} \ , \tag{16}$$

$$\gamma_{xy} = s_{16}\sigma_x + s_{26}\sigma_y + s_{66}\tau_{xy} \ , \tag{17}$$

where ϵ_x, ϵ_y and γ_{xy} are the axial normal strain, transverse normal strain and transverse shear strain, respectively. To obtain the interior strains, we substitute Eqs. (12)–(14) into Eqs. (15)–(17). The strain-displacement relations are

$$\epsilon_x = \frac{\partial U_x}{\partial x} \ , \tag{18}$$

$$\epsilon_y = \frac{\partial U_y}{\partial y} \ , \tag{19}$$

$$\gamma_{xy} = \frac{\partial U_x}{\partial y} + \frac{\partial U_y}{\partial x} \ , \tag{20}$$

where $U_x(x,y)$ and $U_y(x,y)$ are the displacements in the directions of x and y, respectively. The displacements are integrated from Eqs. (18) and (19), and the resulting arbitrary integration functions are solved by substituting the calculated displacements into (20). This standard procedure is described, for example, in [23]. As the result, we get for the general 2D interior displacements the expressions

$$\begin{aligned} U_x &= 2c_1(s_{11}x + s_{16}y) + 3c_2(2s_{11}x + s_{16}y)y + Cy + D_1 + U_x^q \\ &\quad + c_3\left[3s_{11}x^2y + \left(2\frac{s_{16}^2}{s_{11}} - s_{12}\right)y^3 + 3s_{16}\left(\frac{h^2}{4} + y^2\right)x + s_{66}\left(\frac{3}{4}h^2 - y^2\right)y\right] \ , \end{aligned} \tag{21}$$

$$\begin{aligned} U_y &= 2c_1s_{12}y + 3c_2(s_{12}y^2 - s_{11}x^2) - Cx + D_2 + U_y^q \\ &\quad + c_3\left[3s_{12}xy^2 - s_{11}x^3 + 2s_{12}\frac{s_{16}}{s_{11}}y^3 + s_{26}\left(\frac{3}{4}h^2 - y^2\right)y\right] \ , \end{aligned} \tag{22}$$

where U_x^q and U_y^q depend on the particular load at hand and are given in Appendix A. The integration constants C, D_1 and D_2 constitute the degrees of freedom of the anisotropic plane beam as a rigid body. The constant C relates to a small clockwise rotation about the origin and D_1 and D_2 correspond to translations in the directions of x and y, respectively. Note that as soon as the cross-sectional load resultants are available, the coefficients c_1, c_2 and c_3 can be calculated from Eqs. (7)–(9).

2.4. Calculation examples

In this Section, we study four calculation examples, which are presented in Fig. 2. We note that the interior stresses are of main interest here. In the calculation of the displacements, we follow the customary practice, that is, the displacement conditions to solve the constants C, D_1 and D_2 from Eqs. (21) and (22) are chosen so as to imitate the actual conditions at the ends of the beams. To impose true boundary conditions, we would need to model the boundary layer behavior using Papkovich–Fadle eigenfunctions [22].

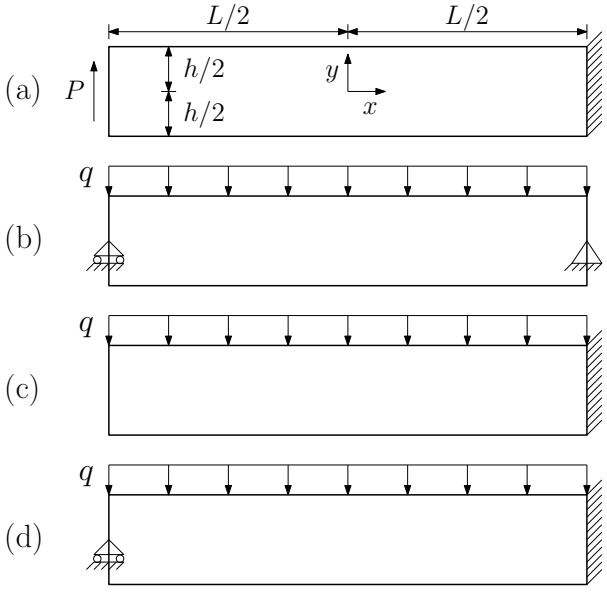

Figure 2: Calculation examples. (a) Cantilever beam subjected to an end-load. (b) Simply-supported beam under a uniform load. (c) Cantilever beam under a uniform load. (d) Propped cantilever beam under a uniform load.

End-loaded cantilever beam. First we consider a cantilever beam subjected to an end-load P at $x = -L/2$ as shown in Fig. 2(a). The structure is statically determinate and the load resultants using the positive

directions of Fig. 1 are

$$N = 0 \ , \ M = -\frac{P(L+2x)}{2} \ , \ Q = -P \ ,$$

from which it follows by Eqs. (7)–(9) that

$$c_1 = \frac{P}{2A}\frac{s_{16}}{s_{11}} \ , \ c_2 = -\frac{PL}{12I} \ , \ c_3 = -\frac{P}{6I} \ .$$

By substituting c_1, c_2 and c_3 into the displacements (21) and (22) and choosing the conditions $U_x(L/2,0) = U_y(L/2,0) = \partial U_x/\partial y(L/2,0) = 0$, the rigid body constants become

$$D_1 = \frac{PLs_{16}}{4A} \ , \quad D_2 = \frac{PL}{48Is_{11}}(5L^2s_{11}^2 - 2h^2s_{16}^2 + 3h^2s_{11}s_{66}) \ ,$$
$$C = \frac{P}{24Is_{11}}(9L^2s_{11}^2 - 2h^2s_{16}^2 + 3h^2s_{11}s_{66}) \ .$$

The strains are obtained from Eqs. (18)–(20) and the stresses by inverting Eqs. (15)–(17), or directly from Eqs. (12)–(14). The axial normal and transverse shear stresses are

$$\sigma_x = -\frac{P}{12Is_{11}}\left[6s_{11}(L+2x)y - s_{16}(h^2 - 12y^2)\right] \ , \quad \tau_{xy} = -\frac{P(h^2-4y^2)}{8I} \ .$$

Fig. 3 shows the relative difference at the centerline ($y = 0$) between the above stresses and those calculated from a 2D plane stress FE model with the boundary conditions $U_x(L/2,y) \equiv U_y(L/2,y) \equiv 0$ using the parameter values $L = 1.6$ m, $h = 0.2$ m, $t = 0.04$ m, $P = -1$ kN. The shear stress reflects the "rule of thumb" used in *isotropic* cases, that is, the interior solution is a good approximation when the axial distance to an end of the beam is at least equal to the height of the beam. However, the axial normal stress given by the 2D FE model starts to deviate from the interior solution well before this limit. It is known that the boundary layer can be thicker in anisotropic than in isotropic cases [24].

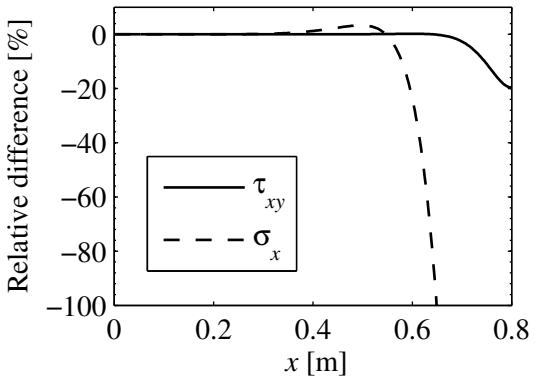

Figure 3: The relative difference between the Airy stresses and those from a 2D FE cantilever model at $y = 0$ with the elastic compliances $s_{11} = 4.49 \cdot 10^{-12}$, $s_{22} = 8.13 \cdot 10^{-12}$, $s_{12} = 9.48 \cdot 10^{-15}$, $s_{16} = -5.84 \cdot 10^{-13}$, $s_{26} = -2.13 \cdot 10^{-13}$ and $s_{66} = 1.31 \cdot 10^{-11}$ m^2/N. The relative difference is calculated from $(\sigma_{x,\mathrm{FE}} - \sigma_{x,\mathrm{Airy}})/\sigma_{x,\mathrm{Airy}} \times 100$.

Simply-supported beam. As another example, let us consider a simply-supported beam under a constant uniform load q according to the configuration presented in Fig. 2(b). The axial force, bending moment and shear force along the beam are given by

$$N(x) = 0 \ , \ M(x) = q\left(\frac{x^2}{2} - \frac{L^2}{8}\right) \ , \ Q(x) = qx \ .$$

We obtain from Eqs. (7)–(9)

$$c_1 = c_3 = 0 \ , \quad c_2 = \frac{q}{240Is_{11}^2}\left[h^2 s_{11}(2s_{12}+s_{66}) - 4h^2 s_{16}^2 - 5L^2 s_{11}^2\right]$$

By substituting c_1, c_2 and c_3 into the displacements (21) and (22), and choosing the conditions $U_x(L/2,0) = U_y(\pm L/2,0) = 0$, we find the rigid body constants to be

$$C = 0 \ , \ D_1 = \frac{qL}{16A}(4hs_{12} - Ls_{16}) \ ,$$
$$D_2 = -\frac{qL^2}{1920Is_{11}}\left[25L^2 s_{11}^2 - 16h^2 s_{16}^2 + 6h^2 s_{11}(3s_{12}+4s_{66})\right] \ .$$

The axial normal and transverse shear stresses are

$$\sigma_x = -\frac{qy}{120Is_{11}^2}\left[15s_{11}^2(L^2-4x^2) + 4s_{16}^2(3h^2-20y^2)\right]$$
$$-\frac{q}{120Is_{11}}\left[s_{12}(40y^3-6h^2y) + 10s_{16}(h^2-12y^2)x + s_{66}(20y^2-3h^2)y\right] \ ,$$
$$\tau_{xy} = \frac{q}{24Is_{11}}(3s_{11}x + 2s_{16}y)(h^2-4y^2) \ .$$

Fig. 4 shows how the above shear stress behaves near the center of the beam. The parameter values are the same as in the previous example with the exceptions of $P = 0$ and $q = 40$ kN/m. Results from a 2D plane stress FE model are also presented. The shear stress distribution is cubic due to anisotropy over the height of the beam at the center but starts to turn quickly into a parabola outside the cross-section $x = 0$.

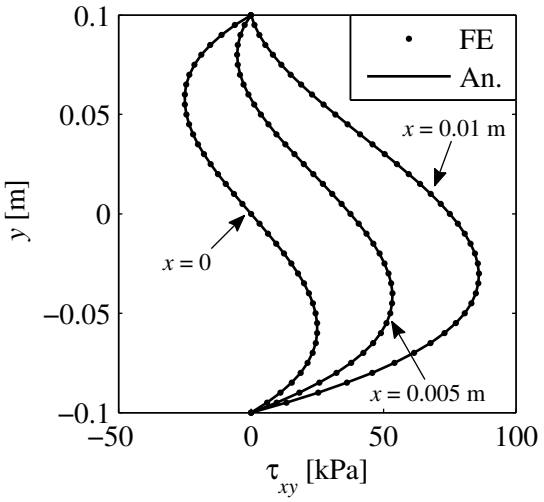

Figure 4: Shear stress distributions near the center of the uniformly-loaded simply-supported beam.

Cantilever beam under uniform load. As a further example, we study a cantilever beam under a uniform load, see Fig. 2(c). It is easy to see that this case can also be solved by the superposition of the two cases presented above by choosing $P = -qL/2$ for the end-loaded cantilever. By superposing the stresses and calculating the load resultants (1), we obtain for the uniformly-loaded cantilever

$$N = 0 \ , \ M = \frac{q(L+2x)^2}{8} \ , \ Q = \frac{q(L+2x)}{2} \ .$$

An instructive discussion on the use of superposition in 2D plane beam problems can be found in [25].

Propped cantilever under uniform load. As the final example, we examine the propped cantilever under a uniform load shown in Fig. 2(d). The load resultants can be written as

$$N = 0 \ , \ M = \frac{q(L+2x)^2}{8} - \frac{F(L+2x)}{2} \ , \ Q = \frac{q(L+2x)}{2} - F \ ,$$

where F is the unknown vertical reaction force at the propped end. The coefficients c_1, c_2 and c_3 are obtained from Eqs. (7)–(9) after which C, D_1, D_2 and F are calculated using the conditions $U_x(L/2,0) = U_y(L/2,0) = \partial U_x/\partial y(L/2,0) = U_y(-L/2,0) = 0$. The reaction force is found as

$$F = \frac{q\left[30L^3 s_{11}^2 - 12h^2 L s_{16}^2 - h^2 s_{11}(9Ls_{12} + 10hs_{26} - 18Ls_{66})\right]}{10\left[8L^2 s_{11}^2 + h^2(3s_{11}s_{66} - 2s_{16}^2)\right]} \ ,$$

after which the calculation of the stresses is straightforward. In conclusion, the general interior solution enables the solution of many 2D plane beam problems in a unified and effortless manner.

3. 2D solution in 1D form

3.1. Third-order kinematics of the beam

The general 2D interior solution studied in Section 2 can be presented in terms of three kinematic variables derived from the displacements (21) and (22) at the central axis of the beam so that the variables depend only on x. We obtain for the axial displacement and the transverse deflection of the central axis, and for the clockwise positive rotation of the cross-section at the central axis the expressions

$$u_x(x) \equiv U_x(x,0) = 2c_1 s_{11} x + \frac{3}{4}h^2 c_3 s_{16} x + D_1 + \frac{qx}{4A}(s_{16}x - 2hs_{12}) \ , \tag{23}$$

$$\begin{aligned} u_y(x) \equiv U_y(x,0) = &- 3c_2 s_{11} x^2 - c_3 s_{11} x^3 - Cx + D_2 \\ &- \frac{qx^2}{48 I s_{11}}\left[2s_{11}^2 x^2 + 4h^2 s_{16}^2 - 3h^2 s_{11}(s_{12} + s_{66})\right] \ , \end{aligned} \tag{24}$$

$$\begin{aligned} \phi(x) \equiv \frac{\partial U_x}{\partial y}(x,0) = &\, 2c_1 s_{16} + 6c_2 s_{11} x + \frac{3}{4}c_3(4x^2 s_{11} + h^2 s_{66}) + C \\ &+ \frac{q}{24 I s_{11}}\left[4x^3 s_{11}^2 + 2h^2 s_{16}^2 x - h^2 s_{11}(3s_{12}x + hs_{26})\right] \ , \end{aligned} \tag{25}$$

respectively. Using these kinematic *central axis variables*, we can present the displacements (21) and (22) of the plane stress state in the form

$$U_x = u_x + y\phi - \frac{4y^3}{3h^2}\left(\phi + \frac{\partial u_y}{\partial x} - \frac{s_{16}}{s_{11}}\frac{\partial u_x}{\partial x}\right) + \frac{y^2}{2}\frac{s_{16}}{s_{11}}\frac{\partial \phi}{\partial x} - \frac{y^3}{6}\left(\frac{s_{12}}{s_{11}} - \frac{s_{16}^2}{s_{11}^2}\right)\frac{\partial^2 \phi}{\partial x^2} + U_x^A \ , \tag{26}$$

$$U_y = u_y + y\frac{s_{12}}{s_{11}}\left(\frac{\partial u_x}{\partial x} + \frac{y}{2}\frac{\partial \phi_x}{\partial x}\right) + \frac{y}{24 s_{11}^2}\left[(8y^2 - 3h^2)s_{12}s_{16} + (3h^2 - 4y^2)s_{11}s_{26}\right]\frac{\partial^2 \phi}{\partial x^2} + U_y^A \ , \tag{27}$$

where the functions U_x^A and U_y^A depend on the applied load and are given in Appendix A. The displacements (26) and (27) represent the exact third-order interior kinematics of a linearly elastic homogeneous anisotropic beam under a uniform load that has a narrow rectangular cross-section. In the isotropic case, the elastic compliances become

$$s_{16} = s_{26} = 0 \ , \ s_{11} = s_{22} = 1/E \ , \ s_{12} = -\nu/E \ , \ s_{66} = 1/G \ , \tag{28}$$

where E and G are the Young's modulus and shear modulus, respectively, and ν is the Poisson ratio. Assuming isotropy, the displacements (26) and (27) simplify to

$$U_x = u_x + y\phi - \frac{4y^3}{3h^2}\left(\phi + \frac{\partial u_y}{\partial x}\right) + \frac{\nu y^3}{6}\frac{\partial^2 \phi}{\partial x^2} \ , \tag{29}$$

$$U_y = u_y - \nu y\frac{\partial u_x}{\partial x} - \frac{\nu y^2}{2}\frac{\partial \phi}{\partial x} + U_y^I \ , \tag{30}$$

where

$$U_y^I = \frac{qy}{48EI}\left[(2h+3y)(\nu^2-1)h^2 + 2y^3(1+2\nu)\right] \ . \tag{31}$$

We see that the Poisson effect (lateral contraction/expansion) is fully included in the displacements (29) and (30). To derive the 2D displacement field in terms of the central axis variables for isotropic material behavior, one may also consider the Marguerre function for the case of plane stress and the Love strain function for plane strain instead of the Airy stress function, see, e.g. [26]. If we neglect the load term and the Poisson effect in Eqs. (29) and (30), the 2D displacement field is exactly of the same form as in the Levinson and Reddy–Bickford beam theories [18–20]. These theories are formulated by assuming that the central axis variables $u_x(x)$, $u_y(x)$ and $\phi(x)$ do not initially take the polynomial forms (23)–(25), but are arbitrary, sufficiently smooth functions. Next, to discuss interior theories in general and the well-known discrepancies between the Levinson and Reddy–Bickford theories, we turn to the energetic aspects of the plane beam.

3.2. Applying Clapeyron's theorem

The strain energy of the 2D anisotropic plane beam and the external work due to the uniform load are given by

$$U = \frac{1}{2}\int_V (\sigma_x\epsilon_x + \sigma_y\epsilon_y + \tau_{xy}\gamma_{xy})dV \ , \quad W_q = -\int_{-L/2}^{L/2} qU_y(x,h/2)dx \ , \tag{32}$$

respectively. While the contributions (32) to the total potential energy of the beam are apparent, the following consideration may not be that obvious at first. We recall from the problem definition in Section 2.1 that the interior solution part represents merely a beam section with fully-developed interior stresses which has been cut off from a complete beam so that the boundary layer is not modeled. Thus, we obtain for the work due to the stresses on the lateral end surfaces of the interior beam

$$\begin{aligned} W_s = {} & t\int_{-h/2}^{h/2} \sigma_x(L/2,y)U_x(L/2,y)dy - t\int_{-h/2}^{h/2} \sigma_x(-L/2,y)U_x(-L/2,y)dy \\ & + t\int_{-h/2}^{h/2} \tau_{xy}(L/2,y)U_y(L/2,y)dy - t\int_{-h/2}^{h/2} \tau_{xy}(-L/2,y)U_y(-L/2,y)dy \ . \end{aligned} \tag{33}$$

By substituting the polynomial expressions according to the general solution presented in Section 2 for σ_x, ϵ_x, σ_y, ϵ_y, τ_{xy}, γ_{xy}, U_x and U_y into (32) and (33), and by handling the laborious calculations by the aid of Mathematica (see the online supplementary file), we find that

$$2U - W_q - W_s = 0 \ . \tag{34}$$

The above calculation shows that in static equilibrium the strain energy of the beam is equal to one-half of the work done by the surface tractions if they were to move (slowly) through their respective displacements. This is exactly according to the *Clapeyron's theorem* (see, e.g. [23]). The recent variational formulation for the Levinson interior beam theory was carried out by accounting for the external virtual work due to the stresses on the end surfaces of the interior beam [21]. The resulting beam equations were exactly the same as those in the case of the vectorial derivation by Levinson [18]. The variational formulation for the Levinson beam theory given in [21] did not actually include the axial displacement $u_x(x)$. With this in mind, let us complement that formulation by the following consideration, which illustrates how consistent equilibrium equations for interior theories can be obtained when employing the principle of virtual displacements.

Example – Variational treatment of a rod with Poisson effect. We study an isotropic interior rod in pure tension so that $M(x) \equiv Q(x) \equiv u_y(x) \equiv \phi(x) \equiv 0$ and $q = 0$. The displacements (29) and (30) are

$$U_x = u_x \ , \quad U_y = -\nu y\frac{\partial u_x}{\partial x} \ , \tag{35}$$

where the central axis variable according to Eqs. (23) and (28) is

$$u_x = U_x(x,0) = \frac{2c_1 x}{E} + D_1 \ . \tag{36}$$

In the following, we want to carry out a variational formulation which leads to the governing differential equation for the axial rod. Our aim is to consider under what conditions the variational procedure leads to the same result as the polynomial Airy stress function method. We assume next that $u_x(x)$ is a sufficiently smooth function, but otherwise arbitrary. We take as the starting point of the variational formulation the displacement field (35) of the rod

$$U_x(x,y) = u_x \ , \qquad U_y(x,y) = -\nu y u_x' \ , \tag{37}$$

where comma denotes diffenrentiation with respect to x. The axial normal and transverse shear stresses are

$$\sigma_x = E\epsilon_x = Eu_x' \ , \qquad \tau_{xy} = G\gamma_{xy} = -G\nu y u_x'' \ . \tag{38}$$

The internal virtual work is

$$\begin{aligned} \delta U &= \int_{-L/2}^{L/2} \int_A (\sigma_x \delta\epsilon_x + \tau_{xy}\delta\gamma_{xy}) dA dx = \int_{-L/2}^{L/2} (N\delta u_x' - \nu S \delta u_x'') dx \\ &= -\int_{-L/2}^{L/2} (N'\delta u_x + \nu S''\delta u_x) dx + [N\delta u_x - \nu S \delta u_x' + \nu S' \delta u_x]_{-L/2}^{L/2} \ , \end{aligned} \tag{39}$$

where the axial force and the higher-order load resultant are given by

$$N = \int_A \sigma_x dA = EAu_x' \ , \qquad S = \int_A \tau_{xy} y dA = -\frac{\nu h^2}{12} GAu_x'' \ , \tag{40}$$

respectively. The external virtual work due to the interior stresses on the lateral end surfaces calculated using (33), (37) and (38) results in

$$\delta W_s = [N\delta u_x - \nu S \delta u_x']_{-L/2}^{L/2} \ . \tag{41}$$

By applying the principle of virtual displacements, $\delta U = \delta W_s$, the equilibrium equation and interior boundary conditions are found as

$$N' + \nu S'' = 0 \qquad \text{and} \qquad [\nu S' \delta u_x]_{-L/2}^{L/2} = 0 \ . \tag{42}$$

Note that the second term on the left-hand side of the equilibrium equation is due to the Poisson effect and that it violates the axial equilibrium condition if it is nonzero. In addition, according to the interior beam definition, the virtual displacement δu_x is free in the interior region, including the interior end surfaces. This means that the interior boundary conditions simplify to

$$\nu S'(\pm L/2) = 0 \ . \tag{43}$$

Next we use (40) and (42) and write

$$f \equiv \nu S' = -\frac{\nu^2 h^2}{12} GAu_x''' \quad \rightarrow \quad f' = -N' = -EAu_x'' \quad \rightarrow \quad f'' = -EAu_x''' \ . \tag{44}$$

It follows that $f'' = \beta^2 f \rightarrow f = \alpha_1 \mathrm{e}^{\beta x} + \alpha_2 \mathrm{e}^{-\beta x}$, where $\beta^2 = 24(1+\nu)/(\nu h)^2$. With the interior boundary conditions (43), that is, $f(\pm L/2) = 0$, we obtain $\alpha_1 = \alpha_2 = 0 \rightarrow f \equiv 0$. Therefore, the equilibrium equation in (42) simplifies to

$$N' = EAu_x'' = 0 \ , \tag{45}$$

which may be compared to the first of (10). The solution to (45) is given by u_x in (36), that is, by the Airy elasticity solution. Note that if the function f above would not vanish, the differential equation for u_x would be of fourth order and its solution would also contain exponential terms. We see that the higher-order load resultant S has no physical meaning in the interior context. We conclude that with the inclusion of the lateral contraction and expansion (the Poisson effect) in the rod model, it becomes apparent that the virtual work due to the interior stresses on the lateral end surfaces of the interior rod is a crucial part of the variational formulation in order to avoid spurious exponential end effects and violation of the axial equilibrium of the rod. Similar conclusions were arrived at in the case of the Levinson beam theory, for details and further discussion, see [21].

3.3. 1D beam equations

Instead of a variational formulation similar to the previous example, we may derive the 1D beam equations directly by using the global equilibrium equations (10). In terms of the polynomial central axis variables (23)–(25), the strains (18)–(20) calculated using the displacements (21) and (22) of the plane stress state can be written as

$$\epsilon_x = \frac{\partial u_x}{\partial x} + y\frac{\partial \phi}{\partial x} + \frac{y^2}{2}\frac{s_{16}}{s_{11}}\frac{\partial^2 \phi}{\partial x^2} + \epsilon_x^A \ , \tag{46}$$

$$\epsilon_y = \frac{s_{12}}{s_{11}}\left(\frac{\partial u_x}{\partial x} + y\frac{\partial \phi}{\partial x}\right) + \frac{1}{8s_{11}^2}\left[(h^2-4y^2)s_{11}s_{26} - (h^2-8y^2)s_{12}s_{16}\right]\frac{\partial^2 \phi}{\partial x^2} + \epsilon_y^A \ , \tag{47}$$

$$\gamma_{xy} = \left(1-\frac{4y^2}{h^2}\right)\left(\phi + \frac{\partial u_y}{\partial x}\right) + \frac{s_{16}}{s_{11}}y\left[\frac{\partial \phi}{\partial x} + y\left(\frac{4}{h^2}\frac{\partial u_x}{\partial x} + \frac{1}{2}\frac{s_{16}}{s_{11}}\frac{\partial^2 \phi}{\partial x^2}\right)\right] + \gamma_{xy}^A \ , \tag{48}$$

where the load-dependent parts ϵ_x^A, ϵ_y^A and γ_{xy}^A are given in Appendix A. Using the strains (46)–(48) and by inverting the plane stress constitutive relations (15)–(17), we can calculate the load resultants (1) in terms of the central axis variables and substitute them into the equilibrium equations (10) to obtain 1D beam equations. For full anisotropic coupling this procedure leads to unwieldy expressions. For the sake of brevity, we consider here only the isotropic case, which can be easily compared to existing 1D beam theories. We apply Eqs. (28) to the strains (46)–(48) and to the constitutive relations (15)–(17), after which the calculation of the load resultants (1) gives

$$N = EA\frac{\partial u_x}{\partial x} - \frac{qh\nu}{2} \ , \tag{49}$$

$$M = EI\frac{\partial \phi}{\partial x} - \frac{qh^2}{40}(2+5\nu) \ , \tag{50}$$

$$Q = \frac{2}{3}GA\left(\phi + \frac{\partial u_y}{\partial x}\right) \ . \tag{51}$$

Substitution of the load resultants into the equilibrium equations (10) leads to

$$EA\frac{\partial^2 u_x}{\partial x^2} = 0 \ , \tag{52}$$

$$EI\frac{\partial^2 \phi}{\partial x^2} - \frac{2}{3}GA\left(\phi + \frac{\partial u_y}{\partial x}\right) = 0 \ , \tag{53}$$

$$\frac{2}{3}GA\left(\frac{\partial \phi}{\partial x} + \frac{\partial^2 u_y}{\partial x^2}\right) = q \ . \tag{54}$$

By uncoupling Eqs. (53) and (54), we obtain alternatively

$$EI\frac{\partial^3 \phi}{\partial x^3} = q \ , \tag{55}$$

$$EI\frac{\partial^4 u_y}{\partial x^4} = -q \ . \tag{56}$$

In summary, the general solution to Eqs. (52)–(54) is given by Eqs. (23)–(25) and (28), and the solution is expanded into the whole interior region of the 2D plane beam through Eqs. (29)–(31). These equations constitute an alternative representation of the elasticity solution presented in Section 2 in the isotropic case. We can see, for example, that the obtained beam equations (55) and (56) are exactly the same as those in the Timoshenko beam theory with a constant uniform distributed load. Eqs. (51) and (54) are the same as in the static Levinson beam theory. 1D beam presentations may be obtained for more complicated loads by updating the load-dependent part (6) of the stress function (5). The provided exact 1D interior presentation enables a more thorough study of the pros and cons of approximate interior beam theories, such as those of Levinson and Timoshenko, on the level of governing differential equations instead of simplistic (numerical) comparisons between specific 2D elasticity and 1D beam solutions.

4. Exact anisotropic beam finite element

4.1. Elasticity solution in terms of FE-degrees of freedom

The general interior displacements (21) and (22) can be used as the basis for the derivation of an exact 1D beam finite element. Similarly to the 1D beam equations given in the previous section, the finite element equations constitute an alternative presentation of the exact 2D interior elasticity solution presented in Section 2. Fig. 5 presents the setting according to which the element is developed. Both nodes in Fig. 5 have three degrees of freedom. For nodes $i = 1, 2$, we have axial displacements $u_{x,i}$, transverse displacements $u_{y,i}$ and rotations ϕ_i. By the aid of the central axis variables (23)–(25), we obtain for nodes 1 and 2 six equations

$$\begin{aligned} u_{x,1} &= u_x(-L/2) \ , & u_{x,2} &= u_x(L/2) \ , \\ u_{y,1} &= u_y(-L/2) \ , & u_{y,2} &= u_y(L/2) \ , \\ \phi_1 &= -\phi(-L/2) \ , & \phi_2 &= -\phi(L/2) \ . \end{aligned} \tag{57}$$

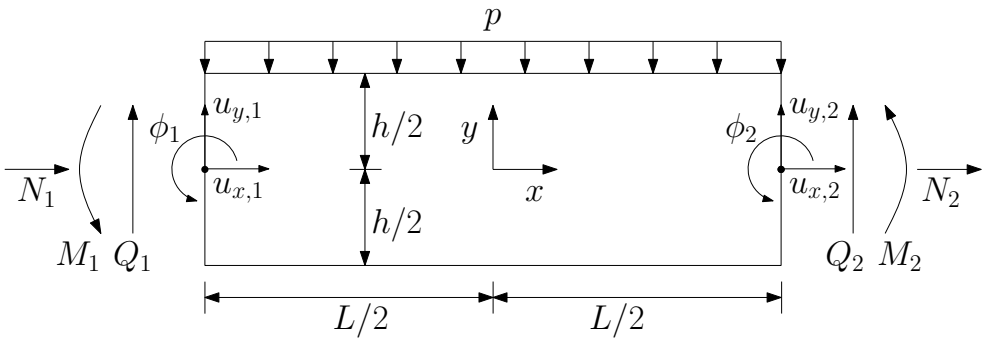

Figure 5: Set-up according to which the exact interior beam finite element is developed.

We can solve the six unknowns c_1, c_2, c_3, C, D_1 and D_2 from Eqs. (57). This results in the following relations

$$\begin{aligned} c_1 &= \frac{3h^2 s_{16}}{4\Delta L}\left[2(u_{y,1}-u_{y,2}) + L(\phi_1+\phi_2)\right] - \frac{2L^2 s_{11} + 3h^2 s_{66}}{2\Delta L}(u_{x,1}-u_{x,2}) \\ &\quad + \frac{q}{4\Delta t}\left[2L^2 s_{11}s_{12} + 3h^2(s_{12}s_{66} - s_{16}s_{26})\right] \ , \\ c_2 &= \frac{\phi_1 - \phi_2}{6Ls_{11}} - \frac{q}{144Is_{11}^2}\left[L^2 s_{11}^2 + h^2(2s_{16}^2 - 3s_{11}s_{12})\right] \ , \\ c_3 &= \frac{4s_{16}}{\Delta L}(u_{x,1}-u_{x,2}) - \frac{2s_{11}}{\Delta L}\left[2(u_{y,1}-u_{y,2}) + L(\phi_1+\phi_2)\right] + \frac{2q}{\Delta t}(s_{11}s_{26} - s_{12}s_{16}) \ , \end{aligned} \tag{58}$$

$$
\begin{aligned}
C &= \frac{3(u_{y,1}-u_{y,2})}{\Delta L}[L^2 s_{11}^2 + h^2(s_{11}s_{66}-s_{16}^2)] + \frac{L^2 s_{11}^2}{2\Delta}(\phi_1+\phi_2) \\
&\quad - \frac{L s_{11} s_{16}}{\Delta}(u_{x,1}-u_{x,2}) - \frac{qL^2 s_{11}}{2\Delta t}(s_{11}s_{26}-s_{12}s_{16}) \ , \\
D_1 &= \frac{u_{x,1}+u_{x,2}}{2} - \frac{qL^2 s_{16}}{16A} \ , \\
D_2 &= \frac{1}{8}\left[4(u_{y,1}+u_{y,2}) + L(\phi_1-\phi_2)\right] - \frac{qL^2}{384 I s_{11}}\left[L^2 s_{11}^2 + h^2(6s_{11}s_{66}-4s_{16}^2)\right] \ ,
\end{aligned}
\tag{59}
$$

where

$$
\Delta = 2L^2 s_{11}^2 + 3h^2(s_{11}s_{66}-s_{16}^2) \ . \tag{60}
$$

By substituting Eqs. (58) and (59) into Eqs. (21) and (22) we can write the 2D displacements in the form

$$
U_x(x,y) = \mathbf{N}_x \mathbf{u} + U_x^F \ , \tag{61}
$$

$$
U_y(x,y) = \mathbf{N}_y \mathbf{u} + U_y^F \ , \tag{62}
$$

where

$$
\mathbf{u} = \left\{ u_{x,1} \quad u_{y,1} \quad \phi_1 \quad u_{x,2} \quad u_{y,2} \quad \phi_2 \right\}^{\mathrm{T}} \tag{63}
$$

is the displacement vector. The shape functions $\mathbf{N}_x$ and $\mathbf{N}_y$ are given in Appendix B, as well as the load-dependent functions U_x^F and U_y^F. Therefore, once the nodal displacements are known, the 2D displacement field can be calculated by substituting them into Eqs. (61) and (62), after which the calculation of the 2D interior strains and stresses is straightforward.

4.2. Finite element equations

To obtain the finite element equations, we substitute Eqs. (58) into Eqs. (7)–(9) to calculate the load resultants at nodes $i = 1, 2$, with the notion that the positive directions are taken to be according to Fig. 1 so that

$$
\begin{aligned}
N_1 &= -N(-L/2) \ , & N_2 &= N(L/2) \ , \\
Q_1 &= -Q(-L/2) \ , & Q_2 &= Q(L/2) \ , \\
M_1 &= M(-L/2) \ , & M_2 &= -M(L/2) \ .
\end{aligned}
\tag{64}
$$

The conventional presentation for the 1D beam element is obtained by writing Eqs. (64) in matrix form. Before doing so, we also derive the FE equations from the total potential energy

$$
\Pi = U - W_q - W_s \ . \tag{65}
$$

The stresses on the end surfaces in Eq. (33) are written as given by Eqs. (12)–(14), where the load resultants are expressed as nodal forces according to Eqs. (64). Then, by calculating (32) and (33) and by applying the principle of minimum total potential energy

$$
\frac{\partial \Pi}{\partial u_{x,i}} = 0 \ , \quad \frac{\partial \Pi}{\partial u_{y,i}} = 0 \ , \quad \frac{\partial \Pi}{\partial \phi_i} = 0 \qquad (i = 1, 2) \tag{66}
$$

we obtain the finite element equilibrium equations. The force-based method and the total potential energy approach result in the same equations, which can be written in the form

$$
\mathbf{K}\mathbf{u} = \mathbf{f} + \mathbf{q} \ . \tag{67}
$$

In explicit form, with $\alpha = 12I/\Delta$, we have

$$\mathbf{K} = \alpha \begin{bmatrix} \frac{A}{\alpha L s_{11}} + \frac{s_{16}^2}{L s_{11}} & -\frac{s_{16}}{L} & -\frac{s_{16}}{2} & -\left(\frac{A}{\alpha L s_{11}} + \frac{s_{16}^2}{L s_{11}}\right) & \frac{s_{16}}{L} & -\frac{s_{16}}{2} \\ -\frac{2s_{16}}{L} & \frac{2s_{11}}{L} & s_{11} & \frac{2s_{16}}{L} & -\frac{2s_{11}}{L} & s_{11} \\ -s_{16} & s_{11} & \frac{\Delta+6L^2 s_{11}^2}{12 L s_{11}} & s_{16} & -s_{11} & -\frac{\Delta-6L^2 s_{11}^2}{12 L s_{11}} \\ -\left(\frac{A}{\alpha L s_{11}} + \frac{s_{16}^2}{L s_{11}}\right) & \frac{s_{16}}{L} & \frac{s_{16}}{2} & \frac{A}{\alpha L s_{11}} + \frac{s_{16}^2}{L s_{11}} & -\frac{s_{16}}{L} & \frac{s_{16}}{2} \\ \frac{2s_{16}}{L} & -\frac{2s_{11}}{L} & -s_{11} & -\frac{2s_{16}}{L} & \frac{2s_{11}}{L} & -s_{11} \\ -s_{16} & s_{11} & -\frac{\Delta-6L^2 s_{11}^2}{12 L s_{11}} & s_{16} & -s_{11} & \frac{\Delta+6L^2 s_{11}^2}{12 L s_{11}} \end{bmatrix} , \tag{68}$$

$$\mathbf{f} = \{N_1 \quad Q_1 \quad M_1 \quad N_2 \quad Q_2 \quad M_2\}^{\mathrm{T}} , \tag{69}$$

$$\mathbf{q} = q \begin{Bmatrix} \frac{2hL^2 s_{11}^2 s_{12} - 2h^3 s_{12} s_{16}^2 - h^3 s_{11}(s_{16} s_{26} - 3 s_{12} s_{66})}{2\Delta s_{11}} \\ -\frac{h^2 s_{16}(2h s_{12} - 3L s_{16}) + 2L^3 s_{11}^2 - h^2 s_{11}(2h s_{26} - 3L s_{66})}{2\Delta} \\ -\frac{1}{120}\left[\frac{2h^2 s_{16}^2}{s_{11}^2} + \frac{3h^2(3s_{12} - s_{66})}{s_{11}} - \frac{60h^3 L s_{11} s_{26}}{\Delta} + 10L^2\left(1 + \frac{6h^3 s_{12} s_{16}}{\Delta L}\right)\right] \\ -\frac{2hL^2 s_{11}^2 s_{12} - 2h^3 s_{12} s_{16}^2 - h^3 s_{11}(s_{16} s_{26} - 3 s_{12} s_{66})}{2 s_{11} \Delta} \\ \frac{h^2 s_{16}(2h s_{12} + 3L s_{16}) - 2L^3 s_{11}^2 - h^2 s_{11}(2h s_{26} + 3L s_{66})}{2\Delta} \\ \frac{1}{120}\left[\frac{2h^2 s_{16}^2}{s_{11}^2} + \frac{3h^2(3s_{12} - s_{66})}{s_{11}} + \frac{60h^3 L s_{11} s_{26}}{\Delta} + 10L^2\left(1 - \frac{6h^3 s_{12} s_{16}}{\Delta L}\right)\right] \end{Bmatrix} . \tag{70}$$

The remarkable feature of Eqs. (67) is the asymmetry of the stiffness matrix (68). The reciprocal theorem [e.g. 22] requires the stiffness matrix to be symmetric. In light of this, the asymmetry of the stiffness matrix can be easily remedied by redefining the generalized axial forces in Eq. (64) as $N_1 \equiv -2N(-L/2)$ and $N_2 \equiv 2N(L/2)$. In other words, if we multiply the first and fourth row of the linear system of equations (67) by a factor of two, the stiffness matrix (68) becomes symmetric. It is also noteworthy that with full anisotropic coupling, every nodal load is associated with every nodal degree of freedom in the end surface work W_s. For example, N_1 is not conjugate only to $u_{x,1}$ in the conventional manner, but also to all the other degrees of freedom. If we were to neglect the interior nature of the plane beam and derive, in the absence of the distributed load, the stiffness matrix in the conventional way on the basis of the strain energy U, we would obtain a symmetric, but incorrect, stiffness matrix. In the isotropic case, the asymmetry of the stiffness matrix (68) vanishes along with the coupling term s_{16} and the equations simplify to

$$\frac{EA}{L}\begin{bmatrix} 1 & -1 \\ -1 & 1 \end{bmatrix}\begin{Bmatrix} u_{x,1} \\ u_{x,2} \end{Bmatrix} = \begin{Bmatrix} N_1 \\ N_2 \end{Bmatrix} + \frac{q\nu h}{2}\begin{Bmatrix} -1 \\ 1 \end{Bmatrix} , \tag{71}$$

$$\frac{EI}{(1+\Phi)L^3}\begin{bmatrix} 12 & 6L & -12 & 6L \\ 6L & (4+\Phi)L^2 & -6L & (2-\Phi)L^2 \\ -12 & -6L & 12 & -6L \\ 6L & (2-\Phi)L^2 & -6L & (4+\Phi)L^2 \end{bmatrix}\begin{Bmatrix} u_{y,1} \\ \phi_1 \\ u_{y,2} \\ \phi_2 \end{Bmatrix} = \begin{Bmatrix} Q_1 \\ M_1 \\ Q_2 \\ M_2 \end{Bmatrix} + \frac{q}{2}\begin{Bmatrix} -L \\ -\frac{10L^2 - 3h^2(2+5\nu)}{60} \\ -L \\ \frac{10L^2 - 3h^2(2+5\nu)}{60} \end{Bmatrix} , \tag{72}$$

where $\Phi = 3h^2(1+\nu)/L^2$. Eqs. (71) and (72) can be written concisely as

$$\mathbf{K}_r \mathbf{u}_r = \mathbf{f}_r + \mathbf{q}_r , \tag{73}$$

$$\mathbf{K}_b \mathbf{u}_b = \mathbf{f}_b + \mathbf{q}_b , \tag{74}$$

where $\mathbf{K}_r$ and $\mathbf{K}_b$ are the rod and beam element stiffness matrices, respectively, and $\mathbf{u}_r$ and $\mathbf{u}_b$ are the rod and beam nodal displacement vectors, respectively. The force vectors are $\mathbf{f}_r$ and $\mathbf{q}_r$ for the rod element, and $\mathbf{f}_b$ and $\mathbf{q}_b$ for the beam element, respectively. Note that the stiffness matrix $\mathbf{K}_b$ is equal to the stiffness matrix of the Levinson beam element and the Timoshenko beam element when the Timoshenko shear coefficient has the value of 2/3 [21, 27]. The presented finite element formalism for the plane beam extends the applicability of the 2D elasticity solution.

5. Conclusions

In this paper, a general interior elasticity solution for a 2D linearly elastic anisotropic plane beam under a uniform load was derived. The exact third-order interior kinematic description for the beam was obtained from the solution. It was shown that in an energy-based formulation, which is founded exclusively on the interior kinematics of the beam, one has to take into account the fact that the interior stresses do work on the lateral end surfaces of the interior beam. A number of higher-order beam theories can be found in the literature that are based exclusively on interior kinematics. However, these higher-order constructions are incomplete as interior beam theories because they lack the aforementioned work due to the stresses at the beam ends.

From a different point of view, the higher-order beam theories attempt to model both the interior part and the boundary layer of a beam simultaneously with the same (interior) kinematic description. In search of an accurate beam theory that would better serve this end, the kinematic description should also include information on the true boundary layer behavior. Adapting the methodology presented in this paper, a kinematic description for the boundary layer may be constructed using Papkovich–Fadle eigenfunctions in association with the Airy stress function [22].

Appendix A. Load-dependent expressions

The load-dependent terms in Eqs. (21) and (22) read

$$\begin{aligned} U_x^q = {} & \frac{q}{6Is_{11}^2}\left(s_{11}^3x^3y + s_{16}^3y^4 - s_{11}^2s_{66}xy^3\right) + \frac{q}{48I}s_{16}\left(h^2+12y^2\right)x^2 \\ & + \frac{q}{24I}\frac{s_{16}}{s_{11}}y\left[s_{12}(h^2-4y^2)y + 2s_{16}(h^2+4y^2)x + s_{66}(h^2-3y^2)y\right] \\ & - \frac{q}{24I}\left[s_{12}(h^3+3h^2y+4y^3)x + s_{26}(h^3+3h^2y-2y^3)y\right] \ , \end{aligned} \tag{A.1}$$

$$\begin{aligned} U_y^q = {} & \frac{q}{48I}\left[3s_{12}(h^2+4y^2)x^2 + s_{22}(2y^3-2h^3-3h^2y)y - 2s_{11}x^4\right] \\ & + \frac{qy}{24I}\frac{s_{16}}{s_{11}}\left[s_{26}(h^2-2y^2)y - 2s_{12}(h^2-4y^2)x\right] + \frac{q}{48I}\frac{s_{66}}{s_{11}}(3h^2s_{11}x^2 - 2s_{12}y^4) \\ & + \frac{q}{24Is_{11}^2}\left[4s_{12}s_{16}^2y^4 - 2s_{11}(s_{12}^2y^4 + h^2s_{16}^2x^2) + s_{11}^2s_{26}(3h^2-4y^2)xy\right] \ . \end{aligned} \tag{A.2}$$

The load-dependent terms in Eqs. (26) and (27) are

$$\begin{aligned} U_x^A = {} & \frac{qy^2}{24Is_{11}}\left[\frac{s_{12}s_{16}}{6}(15h^2+8hy-24y^2) - \frac{s_{16}^3}{s_{11}}(h^2-4y^2)\right. \\ & \left. + s_{16}s_{66}(h^2-3y^2) - \frac{s_{11}s_{26}}{3}(9h^2+4hy-6y^2)\right] \ , \end{aligned} \tag{A.3}$$

$$\begin{aligned} U_y^A = {} & \frac{qy}{24Is_{11}}\left[\frac{s_{12}^2}{2}(2h^3+3h^2y-4y^3) - \frac{s_{11}s_{22}}{2}(2h^3+3h^2y-2y^3)\right. \\ & \left. - \frac{s_{12}s_{16}^2}{s_{11}}y(h^2-4y^2) + s_{16}s_{26}y(h^2-2y^2) - s_{12}s_{66}y^3\right] \ . \end{aligned} \tag{A.4}$$

The load-dependent terms in Eqs. (46)–(48) are given by

$$\epsilon_x^A = \frac{qy^3}{6Is_{11}}\left[2s_{16}^2 - s_{11}(s_{12}+s_{66})\right] , \tag{A.5}$$

$$\epsilon_y^A = \frac{q}{24Is_{11}}\Bigg[s_{12}^2(h^3+3h^2y-8y^3) - s_{11}s_{22}(h^3+3h^2y-4y^3) - 2\frac{s_{12}s_{16}^2}{s_{11}}y(h^2-8y^2) + 2s_{16}s_{26}y(h^2-4y^2) - 4s_{12}s_{66}y^3\Bigg] , \tag{A.6}$$

$$\gamma_{xy}^A = \frac{qy}{24Is_{11}}\Bigg[s_{12}s_{16}(3h^2+4hy-8y^2) - 2\frac{s_{16}^3}{s_{11}}(h^2-8y^2) - s_{11}s_{26}(3h^2+4hy-4y^2) + 2s_{16}s_{66}(h^2-6y^2)\Bigg] . \tag{A.7}$$

Appendix B. Shape functions and load functions

The shape functions in Eqs. (61) and (62) are

$$\mathbf{N}_x^{\mathrm{T}} = \begin{Bmatrix} \frac{2L^2(L-2x)s_{11}^3+16y^3s_{16}^3-3(L-2x)s_{11}^2\left(2(L+2x)ys_{16}-h^2s_{66}\right)-s_{11}s_{16}\left(3h^2(L-2x)s_{16}+8y^2(y(s_{12}+s_{66})-3xs_{16})\right)}{2\Delta Ls_{11}} \\ -\frac{y\left(3\left(L^2-4x^2\right)s_{11}^2-8y^2s_{16}^2-4ys_{11}(3xs_{16}-y(s_{12}+s_{66}))\right)}{\Delta L} \\ \frac{y\left(L(L+6x)(L-2x)s_{11}^3-3h^2ys_{16}^3+s_{11}s_{16}\left(\left(3h^2(L-2x)-8Ly^2\right)s_{16}+3h^2ys_{66}\right)+s_{11}^2\left(4Ly^2s_{12}+2L(L-6x)ys_{16}+\left(4Ly^2-3h^2(L-2x)\right)s_{66}\right)\right)}{2\Delta Ls_{11}} \\ \frac{2L^2(L+2x)s_{11}^3-16y^3s_{16}^3+3(L+2x)s_{11}^2\left(2(L-2x)ys_{16}+h^2s_{66}\right)-s_{11}s_{16}\left(3h^2(L+2x)s_{16}-8y^2(y(s_{12}+s_{66})-3xs_{16})\right)}{2\Delta Ls_{11}} \\ -\frac{y\left(3\left(L^2-4x^2\right)s_{11}^2-8y^2s_{16}^2-4ys_{11}(3xs_{16}-y(s_{12}+s_{66}))\right)}{\Delta L} \\ \frac{y\left(L(L-6x)(L+2x)s_{11}^3+3h^2ys_{16}^3+s_{11}s_{16}\left(\left(3h^2(L+2x)-8Ly^2\right)s_{16}-3h^2ys_{66}\right)+s_{11}^2\left(4Ly^2s_{12}-2L(L+6x)ys_{16}+\left(4Ly^2-3h^2(L+2x)\right)s_{66}\right)\right)}{2\Delta Ls_{11}} \end{Bmatrix} , \tag{B.1}$$

$$\mathbf{N}_y^{\mathrm{T}} = \begin{Bmatrix} \frac{8y^3s_{12}s_{16}^2-s_{11}^2\left(2L^2ys_{12}-x\left(L^2-4x^2\right)s_{16}\right)+ys_{11}\left(\left(3h^2-4y^2\right)s_{16}s_{26}+3s_{12}\left(4xys_{16}-h^2s_{66}\right)\right)}{\Delta Ls_{11}} \\ \frac{2(L-2x)^2(L+x)s_{11}^2+s_{16}\left(2\left(3h^2y-8y^3\right)s_{12}-3h^2(L-2x)s_{16}\right)-s_{11}\left(24xy^2s_{12}+\left(6h^2y-8y^3\right)s_{26}-3h^2(L-2x)s_{66}\right)}{2\Delta L} \\ \frac{L^2-4x^2+4y^2(s_{12}/s_{11})}{8L}+\frac{\left(4x^3-L^2x\right)s_{11}^2+y\left(3h^2-8y^2\right)s_{12}s_{16}-ys_{11}\left(12xys_{12}+\left(3h^2-4y^2\right)s_{26}\right)}{2\Delta} \\ -\frac{8y^3s_{12}s_{16}^2-s_{11}^2\left(2L^2ys_{12}-x\left(L^2-4x^2\right)s_{16}\right)+ys_{11}\left(\left(3h^2-4y^2\right)s_{16}s_{26}+3s_{12}\left(4xys_{16}-h^2s_{66}\right)\right)}{\Delta Ls_{11}} \\ \frac{2(L+2x)^2(L-x)s_{11}^2-s_{16}\left(2\left(3h^2y-8y^3\right)s_{12}+3h^2(L+2x)s_{16}\right)+s_{11}\left(24xy^2s_{12}+\left(6h^2y-8y^3\right)s_{26}+3h^2(L+2x)s_{66}\right)}{2\Delta L} \\ -\frac{L^2-4x^2+4y^2(s_{12}/s_{11})}{8L}+\frac{\left(4x^3-L^2x\right)s_{11}^2+y\left(3h^2-8y^2\right)s_{12}s_{16}-ys_{11}\left(12xys_{12}+\left(3h^2-4y^2\right)s_{26}\right)}{2\Delta} \end{Bmatrix} . \tag{B.2}$$

In addition, in Eqs. (61) and (62) we have the load-dependent terms

$$\begin{aligned} U_x^F = \frac{q}{192\Delta Is_{11}^2}\big\{&24h^2y^2(h^2-4y^2)s_{16}^5 - 4h^2y^2s_{11}s_{16}^3((15h^2+16hy-24y^2)s_{12}+48xys_{16}+6(2h^2-7y^2)s_{66}) \\ &- 16L^2x(L^2-4x^2)ys_{11}^5 + s_{11}^2s_{16}[32h^3y^3s_{12}^2+(3h^4(L^2-4x^2)-4h^2(L^2+36x^2)y^2+64L^2y^4)s_{16}^2 \\ &+ 24h^2y^2(h^2-3y^2)s_{66}^2+8h^2y^2s_{16}((9h^2+8hy-6y^2)s_{26}+36xys_{66})+4h^2y^2s_{12}(24x(y-h)s_{16} \\ &+ (15h^2+8hy-24y^2)s_{66})] - 2s_{11}^4[32L^2xy^3s_{12}+L^2(h^2(L^2-4x^2)+4(L^2-12x^2)y^2)s_{16} \\ &+ 4y((3h^3(L^2-4x^2)+6h^2L^2y-4L^2y^3)s_{26}+x(3h^2(L^2-4x^2)+8L^2y^2)s_{66})] \\ &+ s_{11}^3[8xy(3h^2(L^2-4x^2)+16L^2y^2)s_{16}^2-8h^2y^2s_{66}((9h^2+4hy-6y^2)s_{26}+12xys_{66}) \\ &+ s_{16}(96h^3xy^2s_{26}+(3h^4(4x^2-L^2)+4h^2(L^2+36x^2)y^2-48L^2y^4)s_{66}) \\ &- 8ys_{12}((3h^3(4x^2-L^2)-5h^2L^2y+8L^2y^3)s_{16}+4h^2y^2(hs_{26}+3xs_{66}))]\big\} , \end{aligned} \tag{B.3}$$

$$
\begin{aligned}
U_y^F = \frac{q}{384\Delta I s_{11}^2}\big\{ & 48h^2y^2(h^2-4y^2)s_{12}s_{16}^4 - 2(L^3-4Lx^2)^2 s_{11}^5 + s_{11}^4[16(L^2y((12x^2-L^2)ys_{12} \\
& + (2y^3-2h^3-3h^2y)s_{22}) + x(h^3(L^2-4x^2) + 6h^2L^2y - 8L^2y^3)s_{26}) - 3h^2(5L^4-24L^2x^2+16x^4)s_{66}] \\
& + 4h^2 s_{11}s_{16}^2[2y^2(12y^2-9h^2-16hy)s_{12}^2 + 3s_{16}(h^2(4x^2-L^2)s_{16} - 4y^2(h^2-2y^2)s_{26}) \\
& + 12ys_{12}(2x(h^2-4y^2)s_{16} + y(5y^2-h^2)s_{66})] + 2s_{11}^2[12h^2ys_{12}^2((2h^3+3h^2y-4y^3)s_{66} - 8hxys_{16}) \\
& + 3h^2s_{16}(8y^2(h^2-2y^2)s_{26}s_{66} + s_{16}(4y(2h^3+3h^2y-2y^3)s_{22} + 8xy(4y^2-3h^2)s_{26} \\
& + 5h^2(L^2-4x^2)s_{66})) + 4ys_{12}(y(16L^2y^2 - h^2(36x^2+L^2))s_{16}^2 - 6h^2y^3s_{66}^2 - 12h^2s_{16}(h(h^2-2y^2)s_{26} \\
& + x(h^2-4y^2)s_{66}))] + s_{11}^3[16L^2y(2h^3+3h^2y-4y^3)s_{12}^2 + h^2(11L^4-56L^2x^2+48x^4)s_{16}^2 \\
& + 32L^2y^2(h^2-2y^2)s_{16}s_{26} + 2h^2(8h(3h^2y-4y^3)s_{26}^2 + 12y((2y^3-2h^3-3h^2y)s_{22} \\
& + 2x(3h^2-4y^2)s_{26})s_{66} - 9h^2(L^2-4x^2)s_{66}^2) + 8s_{12}(2x(h^3(4x^2-L^2) \\
& - 4h^2L^2y + 16L^2y^3)s_{16} + y^2(24h^3xs_{26} + (3h^2(12x^2-L^2) - 4L^2y^2)s_{66}))]\big\}. \qquad \text{(B.4)}
\end{aligned}
$$

References

[1] Lekhnitskii SG. Theory of elasticity of an anisotropic body. San Francisco: Holden–Day; 1963.
[2] Stroh AN. Dislocations and cracks in anisotropic elasticity. Philos Mag 1958;3(30):625–46.
[3] Stroh AN. Steady–state problems in anisotropic elasticity. J Math Phys 1962;41(2):77–103.
[4] Silverman IK. Orthotropic beams under polynomial loads. J Engng Mech Div ASCE 1964;90(5):293–319.
[5] Hashin Z. Plane anisotropic beams. J App Mech 1967;34(2):257–63.
[6] Ding HJ, Huang DJ, Wang HM. Analytical solution for fixed-fixed anisotropic beam subjected to uniform load. Appl Math Mech 2006;27(10):1305–10.
[7] Ding HJ, Huang DJ, Chen WQ. Elasticity solutions for plane anisotropic functionally graded beams. Int J Solids Struct 2007;44(1):176–96.
[8] Giavotto V, Borri M, Mantegazza P, Ghiringhelli G, Carmaschi V, Maffioli GC, Mussi F. Anisotropic beam theory and applications. Comput Struct 1983;16(1):403–13.
[9] Bauchau OA. A beam theory for anisotropic materials. J Appl Mech 1985;52(2):416–22.
[10] Berdichevsky V, Armanios E, Badir A. Theory of anisotropic thin-walled closed-cross-section beams. Compos Eng 1992;2(5):411–32.
[11] Murakami H, Reissner E, Yamakawa J. Anisotropic beam theories with shear deformation. J Appl Mech 1996;63(3):660–8.
[12] Yu W, Hodges DH, Volovoi VV, Fuchs ED. A generalized Vlasov theory for composite beams. Thin Wall Struct 2005;43(9):1493–511.
[13] Yu W, Hodges DH, Ho JC. Variational asymptotic beam sectional analysis–an updated version. Int J Eng Sci 2012;59:40–64.
[14] Hodges DH. Nonlinear composite beam theory. Reston, US: American Institute of Aeronautics and Astronautics; 2006.
[15] Jemielita G. On kinematical assumptions of refined theories of plates – a survey. J Appl Mech 1990;57(4):1088–91.
[16] Reddy JN. A general nonlinear 3rd–order theory of plates with moderate thickness. Int J Nonlin Mech 1990;25(6):677–86.
[17] Reddy JN. Mechanics of Laminated Composite Plates and Shells: Theory and Analysis. Boca Raton, Florida: CRC Press; 2nd ed.; 2003.
[18] Levinson M. A new rectangular beam theory. J Sound Vib 1981;74(1):81–7.
[19] Bickford W. A consistent higher order beam theory. Dev Theor Appl Mech 1982;11:137–50.
[20] Reddy JN. A simple higher–order theory for laminated composite plates. J Appl Mech 1984;51(4):745–52.
[21] Karttunen AT, von Hertzen R. Variational formulation of the static Levinson beam theory. Mech Res Commun 2015;66:15–9.
[22] Barber JR. Elasticity. New York: Springer; 3rd ed.; 2010.
[23] Sadd MH. Elasticity – Theory, Applications and Numerics. Oxford: Academic Press; 3rd ed.; 2014.
[24] Horgan CO. Recent developments concerning Saint–Venant's principle: an update. Appl Mech Rev 1989;42(11):295–303.
[25] Doghri I. Mechanics of deformable solids. Berlin: Springer; 2000.
[26] Soutas-Little RW. Elasticity. New York: Dover; 1973.
[27] Kosmatka JB. An improved two–node finite element for stability and natural frequencies of axial–loaded Timoshenko beams. Comput Struct 1995;57(1):141–9.